ANALYSIS OF OPEN LOOP HIGHER HARMONIC CONTROL AT HIGH AIRSPEEDS ON A MODERN FOUR-BLADED ARTICULATED ROTOR

Sesi Kottapalli and Jane Leyland
Rotorcraft Aeromechanics Branch
NASA Ames Research Center
Moffett Field, California

Abstract

The effects of open loop higher harmonic control (HHC) on rotor hub loads, performance, and push rod loads of a Sikorsky S-76 helicopter rotor at high airspeeds (up to 200 knots) and moderate lift (10,000 lb) have been studied analytically. The present analysis was performed as a part of a wind tunnel pre-test prediction and preparation procedure, as well as to provide analytical results for post-test correlation efforts. The test associated with this study is to be conducted in the 40- by 80-Foot Wind Tunnel of the National Full-Scale Aerodynamics Complex (NFAC) at the NASA Ames Research Center. The results from this analytical study show that benefits from HHC can be achieved at high airspeeds. These results clear the way for conducting (with the requirement of safe pushrod loads) an open loop HHC test at high airspeeds in the 40- by 80-Foot Wind Tunnel using an S-76 rotor as the test article.

Introduction

Higher harmonic control (HHC) is one of the several active control concepts that have the goal of reducing helicopter vibration. HHC has been researched, flight and wind tunnel tested by several investigators and organizations.[1-15] To date, due to various adverse considerations (weight, cost, reliability, complexity, etc.), HHC has not yet been implemented in a production helicopter. One possible research avenue would be to successfully test a full-scale, modern, moderate lift rotor at high airspeeds with HHC installed; these airspeeds would presumably exceed those that have been involved in previous full-scale testing. With this additional, high airspeed demonstration of the HHC concept, perhaps future trade-off studies comparing HHC to other vibration reduction methods will conclude that HHC is indeed a viable progressive alternative to existing vibration control methods for implementation on a production helicopter.

Open loop HHC testing involving a 44-ft-diameter Sikorsky S-76 articulated rotor is to be conducted in the 40- by 80-Foot Wind Tunnel at airspeeds up to 200 knots and a thrust level of 10,000 lb. This test would be the first of its kind due its unique combination of airspeed, thrust, and full-scale characteristics.

Analytical Model

The comprehensive rotorcraft analysis code CAMRAD/JA[16] was used to calculate the pushrod loads, fixed system hub loads, and the rotor lift to drag ratio, L/D. The various features of the S-76 analytical aeroelastic model are given below.

As noted earlier, CAMRAD/JA was used to analytically model the four-bladed S-76 rotor mounted on the NASA Ames Rotor Test Apparatus (RTA). The fixed system properties that were considered were those of the NFAC 80- by 120-Foot Wind Tunnel and not those of the NFAC 40- by 80-Foot Wind Tunnel. Unpublished analytical work performed at NASA Ames shows conclusively that due to the inherently sound design of the two support systems (coupled with the RTA) that are associated with these wind tunnels, the rotor parameters of interest (hub loads) are not sensitive to the support system modelling. This implies that the NFAC 80-by 120-Foot and 40- by 80-Foot Wind Tunnel support systems correctly approximate a fixed hub configuration.

The following describes the analytical model exercised in CAMRAD/JA for the present application. A free wake model was used at all airspeeds (40 to 200 knots). The trim procedure simulated wind tunnel trim; the thrust was specified (10,000 lb) with the shaft angle varying with airspeed, and with zero first harmonic flapping. The present trim parameters are given in Table 1. On the structural side, the S-76 blade was modelled by four bending modes (with frequencies 2.72P, 4.72P, 4.97P, and

12.91P) and 2 torsion modes (5.84P, 10.72P). In CAMRAD/JA, force integration (for example, Refs. 17 and 18) was selected as the method to calculate loads. A static stall model was used with table look-up for the S-76 airfoil data. Appendix 1 contains a listing of the CAMRAD/JA input stream for the S-76 rotor as modelled in the present application.

Even though it is the airframe vibrations that are of primary interest, it is assumed that a uniform reduction in the fixed system hub loads will lead to a gradual lessening of the vibrations created by these hub loads. Undoubtedly, there exist helicopter designs which, perhaps due to phasing idiosyncrasies, may experience increased vibration at some fixed system locations even though the hub loads have been made smaller. Nevertheless, the safest approach would be to attempt to reduce the hub loads in a uniform manner. In this study, the fixed system 4P hub shears are taken as the parameters that are to be reduced by HHC.

In the analysis each nP HHC input is assumed to be in the rotating system and is defined as: amplitude * sin(n*Psi + Phase), where the amplitude is in degrees, Psi is the azimuthal coordinate, and Phase is the input phase in degrees. The HHC harmonic "n" takes on the individual values of 3, 4 or 5.

Considerations for the Test Envelope

As might be expected, the high airspeed environment raises immediate concern about one aspect of HHC, namely, the increase in pushrod loads when the control system is operating under conditions in which HHC is active. The present pre-test analysis addresses this safety concern by first correlating existing experimental data on pushrod loads with present analytical predictions and then studying the analytical HHC loads for the test conditions. Briefly, the present analytical results (given later) show that the pushrod load endurance limit is exceeded only at the highest airspeeds in the planned test envelope. Based on these limits, the test envelope may be restricted to airspeeds below 200 knots. Note that the RTA control system should be able to generate the required 1 deg (or smaller) HHC input.

Results

Pushrod Load Trends

Figure 1 shows the correlation of the S-76 pushrod loads from a 1977 test in the 40- by 80-Foot Wind Tunnel[19] and from the present analysis. The correlation is reasonable.

The pushrod load trends as predicted by analysis are shown in Figs. 2 to 4 for varying high airspeeds, HHC phase, and HHC harmonic (3P or 4P or 5P). Considering that the flight test of reference 6 showed that an optimum HHC setting is one that is predominantly composed of 3P input, it is encouraging to see from these figures that it is the 4P input that causes the maximum increase in pushrod loads, with the 3P and 5P inputs resulting in only slight increases over the endurance limit. Although reference 6 considered airframe vibration whereas the present study considers hub loads, one would expect that the character of the optimum setting (3P and a small amount of 5P input) would not vary radically for the same rotor system, the S-76.

In order to obtain a summary view of the pushrod load increase due to HHC, a survey was conducted of the pushrod loads with HHC active (1 deg input at four different phase values 0, 90, 180, and 270 deg). The data base here is the same as that in Figs. 2 to 4. Figures 5 to 7 each show three summary trends with airspeed: 1) baseline pushrod loads; 2) pushrod loads resulting from an "optimum" HHC setting; and 3) The maximum pushrod loads with HHC active. The "optimum" setting is defined as that phase which minimizes the inplane shears. The S-76 pushrod endurance limit of 760 lb is also shown.

Hub Shear Trends

The trends of the baseline (no HHC) inplane shears with airspeed are shown in Fig. 8. It is the high airspeed regime, 140 to 200 knots, that is of interest here. HHC at airspeeds up to approximately 140 knots has been explored in flight .[6]

For the S-76, the inplane shears contribute substantially to the airframe vibration (and hence the presence of the 3P and 5P inplane bifilars on the production S-76 aircraft hub). Also, in the flight test of reference 6 these bifilars were rendered inoperative thus allowing for HHC to be the only vibration reduction mechanism. Therefore, for the present wind tunnel test with the S-76 rotor as the test article and without any bifilars installed, the 4P fixed system inplane shears should be taken as the parameters that are to be minimized.

Accordingly, Figs. 9 and 10 show the effect of optimum ("optimum" has been defined earlier as that phase setting of a 1-deg HHC input which results in minimum inplane shears) 3P HHC on the S-76 longitudinal and

lateral shears. Note that these predicted shears and the benefits due to HHC are both sufficiently large that they can be clearly measured by the RTA steady/dynamic rotor balance system. The analysis predicts that benefits due to HHC are maintained at high airspeeds for this modern rotor system. Also, a comparison of these figures with Fig. 9 of Ref. 6 (which shows the S-76 airframe cockpit centerline vibration variation with airspeed) lends some support to the present analytical results in that the trends with and without HHC are roughly parallel to each other (in all three figures). The trends are parallel because the HHC amplitude is kept constant: 1 deg in the present case and approximately 0.7 deg in the flight test of Ref. 6.

For completeness, the vertical shear, which is initially smaller than the inplane shears, is shown in Fig. 11. This shear increases slightly for an optimum 3P HHC input that minimizes the inplane shears.

For completeness, the rest of this set of open loop HHC trends are shown in Figs. 12 to 14 for the 4P input and Figs. 15 to 17 for the 5P input. Generally, these figures show the same trends as for the 3P input case (with HHC benefits being maintained at high airspeeds). Figure 16 is an exception in that the lateral shear increases due to a 5P input that minimizes the longitudinal shear.

Rotor Performance (Lift/Drag)

The baseline trend of the S-76 rotor lift/drag (L/D) with airspeed is given in Fig. 18. With this baseline prediction, the L/D trend with HHC active (optimum HHC input for minimum inplane shears) was studied. A small benefit is predicted due to a 3P HHC input that minimizes inplane shears (Fig. 19) with a sizeable benefit being predicted at high airspeeds due to a 4P input (Fig. 20). Figure 21 shows that a 5P input does not result in any significant L/D benefits.

Concluding Remarks

The results from this analytical study show that benefits from HHC can be achieved at high airspeeds. These results clear the way for conducting with a safe pushrod load, open loop HHC testing of the S-76 rotor in the 40- by 80-Foot Wind Tunnel at airspeeds up to 200 knots. Analytical results for a post-test correlation effort are in place.

Appendix 1. CAMRAD/JA Input Stream for the S-76 Rotor

```
$NLRTR
TITLE   = 'S-76 HEL','ICOPTER ','MAIN ROT',
          'OR, SWEP','T/TAPERE','D TIP   ',
TYPE    = 'MAIN    ',
RADIUS  =  22.00000    ,
NBLADE  =           4,
SIGMA   =  7.4759997E-02,
ROTATE  =           1,
VTIPN   =  675.00      ,
MHHC    =           0,
THHC    = 20*0.0000000E+00,
THHS    = 20*0.0000000E+00,
MHHCF   =           0,
TOHHC   = 10*0.0000000E+00,
TOHHS   = 10*0.0000000E+00,
TCHHC   = 10*0.0000000E+00,
TCHHS   = 10*0.0000000E+00,
TSHHC   = 10*0.0000000E+00,
TSHHS   = 10*0.0000000E+00,
MHHAF   =           0,
FHHC    = 50*0.0000000E+00,
FHHS    = 50*0.0000000E+00,
BTIP    =           0.990,
OPTIP   =           1,
LINTW   =           0,
TWISTL  =           0.000,
RGMAX   =           0.140,
OPUSLD  =           2,
OPCOMP  =           1,
OPREYN  =           0,
EXPRED  =           0.000,
EXPREL  =           0.000,
OPCFD   =           0,
LDMCFD  =           0,     0,     0,
OPSTLL  =           1,
OPYAW   =           0,
ADELAY  =          15.000,
AMAXNS  =           4.000,
TAU     =        3*-1.000,
PSIDS   =        3*15.000,
ALFDS   =        3*15.000,
ALFRE   =        3*12.000,
CLDSP   =           2.000,
CDDSP   =           0.000,
CMDSP   =          -0.650,
INFLOW  =           1,    0,     0,     0,     0,     0,
KHLMDA  =           1.100,
KFLMDA  =           1.700,
OPFFLI  =           1,
KXLMDA  =           0.000,
KYLMDA  =           0.000,
FXLMDA  =           1.000,
FYLMDA  =           1.000,
```

Appendix 1. Continued

```
FMLMDA  =           1.000,
KINTH   =           0.000,
KINTF   =           0.000,
KINTWB  =           1.500,
KINTHT  =           1.800,
KINTVT  =           0.000,
FACTWU  =           0.500,
OPTZT   =           0,
CTSTZT  =           0.000,
HINGE   =           2,
RCPL    =           1.000,
EFLAP   =           0.037880,
ELAG    =           0.037880,
KFLAP   =        1192.000,
KLAG    =        1192.000,
TSPRNG  =           0.000,
RCPLS   =           0.000,
RFA     =           0.0400,
MRB     =          60,
MRM     =          50,
EPMODE  =           0.5000,
NONROT  =           0,
NCOLB   =           6,
NCOLT   =           3,
NUGC    =  0.0000000E+00,
NUGS    =  0.0000000E+00,
GDAMPC  =  0.0000000E+00,
GDAMPS  =  0.0000000E+00,
TDAMPO  =  0.0000000E+00,
TDAMPC  =  0.0000000E+00,
TDAMPR  =  0.0000000E+00,
WTIN    =           1,
FTO     =  0.0000000E+00,
FTC     =  0.0000000E+00,
FTR     =  0.0000000E+00,
KTO     =   24000.00    ,
KTC     =   24000.00    ,
KTR     =   24000.00    ,
LDAMPC  =   6000.00    ,
LDAMPM  =       0.0    ,
LDAMPR  =  0.1190000    ,
GSB     =10*1.000000E-02,
GST     = 5*1.000000E-02,
MBLADE  =  -1.000000    ,
MASST   =  0.0000000E+00,
XIT     =  0.0000000E+00,
KPIN    =           2,
PHIPH   =  -20.00000    ,
PHIPL   =  0.0000000E+00,
RPB     =  4.5430000E-02,
RPH     =  4.5430000E-02,
XPH     = -2.4640000E-02,
ATANKP  =10*0.0000000E+00,
```

Appendix 1. Continued

```
DEL3G   =  0.0000000E+00,
ZFA     =  0.0000000E+00,
XFA     =  0.0000000E+00,
CONE    =  0.0000000E+00,
DROOP   =  0.0000000E+00,
SWEEP   =  0.0000000E+00,
FDROOP  =  0.0000000E+00,
FSWEEP  =  0.0000000E+00,
OPHVIB  =           1,          0,          1,
FACTM   =   0.7         ,
MRA     =          15,
RAE     =    0.1400000    ,  0.2800000    ,  0.3900000    ,  0.4900000    ,
             0.5800000    ,  0.6600000    ,  0.7300000    ,  0.7900000    ,
             0.8400000    ,  0.8800000    ,  0.9100000    ,  0.9350000    ,
             0.9550000    ,  0.9700000    ,  0.9850000    ,  1.0000000    ,
          15*0.0000000    ,
CHORD   = 8*0.0592700    ,4*0.058730     ,  0.055360     ,  0.043630     ,
             0.0397300    ,              15*0.000000     ,
TWISTA  =    3.300000     ,  4.150000     ,  3.100000     ,  2.150000     ,
             1.300000     ,  0.550000     , -0.100000     , -0.650000     ,
            -1.100000     , -1.450000     , -1.725000     , -1.950000     ,
            -2.125000     , -2.275000     , -2.425000     ,15*0.000000    ,
THETZL  =    1.200000     ,6*1.400000     ,8*0.300000     ,15*0.000000    ,
XA      =  12*-0.000290    ,  0.001600     ,  0.010100     ,  0.018600     ,
           15*0.000000    ,
XAC     =  12*-0.000290    ,  0.001600     ,  0.010100     ,  0.018600     ,
           15*0.000000    ,
ASWEEP  =  12*0.000000    ,3*30.0000000   ,15*0.0000000   ,
MCORRL  =  12*1.000000    ,  0.8500000    ,  0.8400000    ,  0.8200000    ,
           15*0.000000    ,
MCORRD  =  12*1.000000    ,  0.8500000    ,  0.8400000    ,  0.8200000    ,
           15*0.000000    ,
MCORRM  =  12*1.000000    ,  0.8500000    ,  0.8400000    ,  0.8200000    ,
           15*0.000000    ,
DELCD   =  30*0.000000    ,
DELCM   =  30*0.000000    ,
RETAB1  =  30*0.000000    ,
MRI     =          17,
RI      =    0.0000000    ,  0.0649000    ,  0.1406000    ,  0.2462000    ,
             0.3409000    ,  0.4167000    ,  0.4925000    ,  0.5683000    ,
             0.6441000    ,  0.7104000    ,  0.7672000    ,  0.8145000    ,
             0.8619000    ,  0.9208000    ,  0.9636000    ,  0.9882000    ,
             1.0000000    ,34*0.0000000   ,
TWISTI  =  2*0.0000000    ,   2.040000    ,   4.450000    ,   4.090000    ,
              3.330000    ,   2.580000    ,   1.820000    ,   1.060000    ,
              0.400000    , -0.1700000    , -0.6400000    ,  -1.120000    ,
             -1.710000    ,  -2.130000    ,  -2.380000    ,  -2.500000    ,
           34*0.000000    ,
MASS    =  2*0.2740000    ,  0.2520000    ,  0.1040000    , 2*0.1020000   ,
             0.1090000    ,  0.1310000    ,  0.1370000    ,   0.1380000   ,
             0.1500000    ,2*0.1210000    ,  0.1970000    ,   0.0810000   ,
           2*0.0410000    ,34*0.0000000   ,
```

Appendix 1. Concluded

```
XI      = 2*0.0000000   ,  0.0036000   ,  0.0025000   , 2*0.0026000  ,
            0.0080000   ,  0.0011000   , -0.0022000   ,2*-0.0027000  ,
            0.0001200   ,  0.0000000   ,  0.0006000   ,   0.0072000  ,
          2*0.0193000   ,              34*0.0000000   ,
XC      = 2*0.0000000   , -0.0037900   ,  0.0000800   ,   0.0001700  ,
            0.0001500   ,  0.0001000   ,  0.0000800   , 2*0.0000600  ,
          4*0.0006400   ,  0.0019700   ,  0.0108700   ,   0.0108700  ,
         34*0.0000000   ,
KP2     = 2*0.0000100   ,  0.0000900   ,  0.0002100   , 3*0.00020000 ,
          2*0.0001800   ,3*0.0001900   ,  0.0002000   ,   0.00015000 ,
            0.0001800   ,2*0.0004600   ,               34*0.00000000 ,
EIZZ    =  2*80600.00   ,   150500.0   ,    67300.00   ,   51100.00    ,
             41600.00   , 3*37500.00   ,    39400.00   ,   39700.00    ,
             38300.00   ,    36900.00   ,    36600.00   ,   20800.00    ,
            2*7600.00   ,     34*0.00   ,
EIXX    =     2*80000.  ,    1059000.  ,    1616000.   ,   1615000.    ,
             1612000.   , 3*1566000.   , 2*1722000.    ,   1667000.    ,
             1378000.   ,    1440000.  ,    1006000.   , 2*419000.     ,
                34*0.   ,
ITHETA  = 2*1.4000000E-03,  1.1220000E-02,  1.0290000E-02,  9.9100000E-03,
            9.7000000E-03,  1.0520000E-02,  1.1540000E-02,  1.1780000E-02,
            1.2720000E-02,  1.3650000E-02,  1.1350000E-02,  1.1790000E-02,
            1.4750000E-02,  7.0000000E-03,2*9.0000000E-03,
         34*0.0000000E+00,
GJ      = 2*104200.00   ,  112500.00   ,    78500.00   ,   62600.00    ,
             52400.00   , 3*48600.00   ,    49500.00   ,   49700.00    ,
             48700.00   ,    47800.00  ,    47300.00   ,   21500.00    ,
            2*6800.00   ,     34*0.00   ,
$END
```

References

[1]McCloud, J. L., III and Weisbrich, A. L., "Wind-Tunnel Results of a Full-Scale Multicyclic Controllable Twist Rotor." 34th Annual Forum of The American Helicopter Society, May 1978.

[2]Chopra, I. and McCloud, J. L., III, "A Numerical Simulation Study of Open-Loop, Closed-Loop and Adaptive Multicyclic Control Systems." Journal of the American Helicopter Society, January 1983, Vol. 28, No. 1, pp. 63-77.

[3]Shaw, J., Albion, N., Hanker, E. J., and Teal, R. S., "Higher Harmonic Control: Wind Tunnel Demonstration of Fully Effective Vibratory Hub Suppression." 41st Annual Forum of the American Helicopter Society, May 1985.

[4]Wood, E. R., Powers, R. W., Cline, J. H., and Hammond, C. E., "On Developing and Flight Testing a Higher Harmonic Control System." Journal of the American Helicopter Society, Jan. 1985, Vol. 30, No. 1.

[5]O'Leary, J. J., Kottapalli, S. B. R., and Davis, M., "Adaptation of a Modern Medium Helicopter (Sikorsky S-76) to Higher Harmonic Control." NASA CP-2400, Rotorcraft Dynamics 1984, Nov. 1985.

[6]Miao, W., Kottapalli, S. B. R., and Frye, H. M., "Flight Demonstration of Higher Harmonic Control (HHC) on the S-76." 42nd Annual Forum of the American Helicopter Society, June 1986.

[7]Robinson, L. and Friedmann, P. P., "Analytic Simulation of Higher Harmonic Control Using a New Aeroelastic Model." AIAA Paper 89-1321, 1989.

[8]Nguyen, K. and Chopra, I., "Application of Higher Harmonic Control (HHC) to Rotors Operating at High Speed and Maneuvering Flight." 45th Annual Forum of the American Helicopter Society, May 1989.

[9]Lehmann, G., "The Effect of Higher Harmonic Control (HHC) on a Four-Bladed Hingeless Model Rotor." Vertica, Vol. 9, No. 3, 1985, pp. 273-284.

[10]Lehmann, G., "A Digital System for Higher Harmonic Control of a Model Rotor." 8th European Rotorcraft Forum, Paper No. 10.1, 1982.

[11]Polychroniadis, M. and Achache, M., "Higher Harmonic Control: Flight Tests of an Experimental System on a SA 349 Research Gazelle." 42nd Annual Forum of the American Helicopter Society, June 1986.

[12]Kube, R., "New Aspects of Higher Harmonic Control at a Four Bladed Hingeless Model Rotor." 15th European Rotorcraft Forum, Paper No. 43, 1989.

[13]Splettstoesser, W. R., Lehmann, G., and Van Der Wall, B., "Initial Results of a Model Rotor Higher Harmonic Control (HHC) Wind Tunnel Experiment on BVI Impulsive Noise Reduction." 15th European Rotorcraft Forum, Paper No. 01, 1989.

[14]Sopher, R., Studwell, R. E., Cassarino S., Kottapalli, S. B. R., "Coupled Rotor/Airframe Vibration Analysis." NASA CR-3582, Nov. 1982.

[15]Walsh, D., "Flight Test of an Open Loop Higher Harmonic Control System on an S-76A Helicopter." 42nd Annual Forum and Technology Display of the American Helicopter Society, June 1986.

[16]Johnson, W., CAMRAD/JA. "A Comprehensive Analytical Model of Rotorcraft Aerodynamics and Dynamics." Johnson Aeronautics, Palo Alto, California, 1988.

[17]Bielawa, R. L., "Blade Stress Calculations - Mode Deflection vs. Force Integration." Journal of the American Helicopter Society, Vol. 23, No. 3, July 1978.

[18]Hansford, R. E., "A Unified Formulation of Rotor Load Prediction Methods." Journal of the American Helicopter Society, Vol. 31, No. 2, April 1986.

[19]Johnson, W., "Performance and Loads Data From a Wind Tunnel Test of a Full-Scale Rotor With Four Blade Tip Planforms." NASA TM-81229, Sept. 1980. Also USAAVRADCOM TR 80-A-9.

Table 1 CAMRAD/JA trim parameters for the present S-76 application (positive series for the cyclics, negative shaft angle represents downward tilt)

Airspeed, knots	Collective, deg	Cos cyclic, deg	Sin cyclic, deg	Shaft angle, deg
80	7.79	–2.69	1.32	–1.29
140	10.32	–2.52	2.57	–3.95
160	11.93	–2.48	3.69	–5.16
180	14.11	–2.82	4.99	–6.54
200	16.80	–3.67	6.40	–8.08

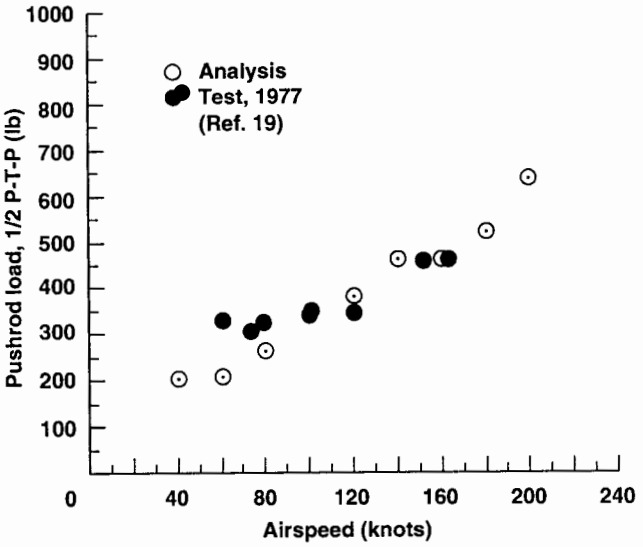

Fig. 1 Correlation of pushrod loads, S-76, 10,000 lb.

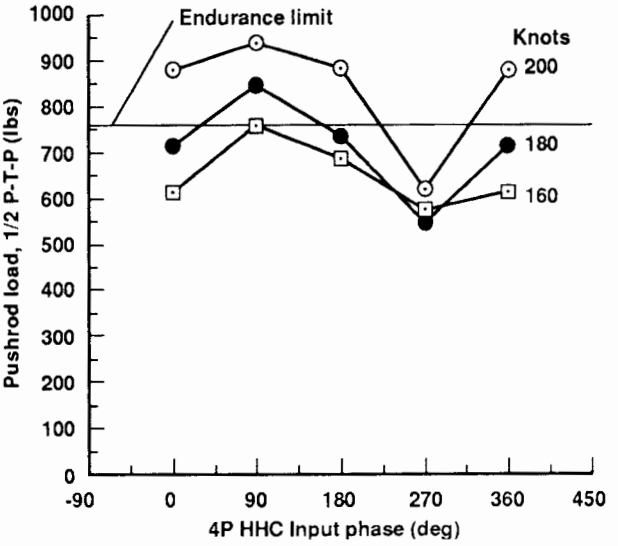

Fig. 3 Variation of pushrod load with 1 deg 4P HHC input phase and airspeed, S-76, 10,000 lb.

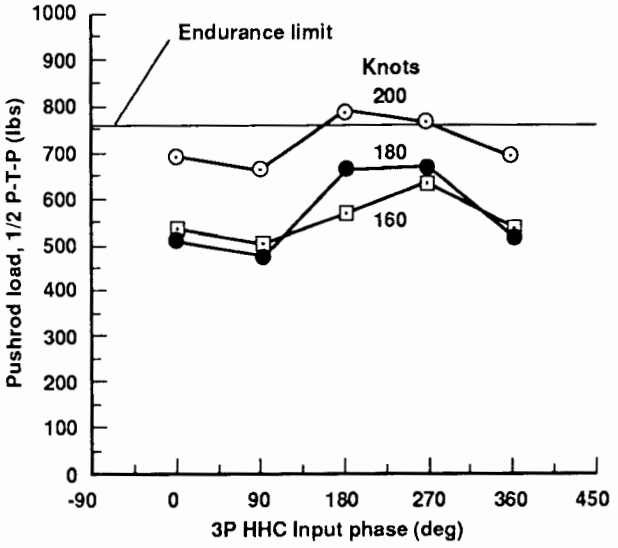

Fig. 2 Variation of pushrod load with 1 deg 3P HHC input phase and airspeed, S-76, 10,000 lb.

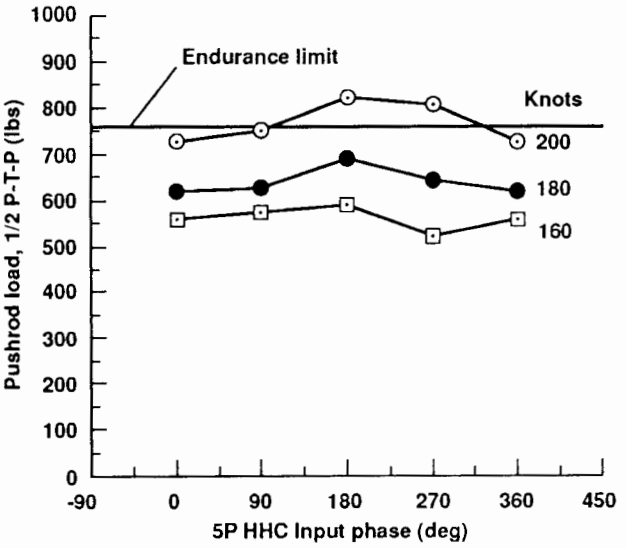

Fig. 4 Variation of pushrod load with 1 deg 5P HHC input phase and airspeed, S-76, 10,000 lb.

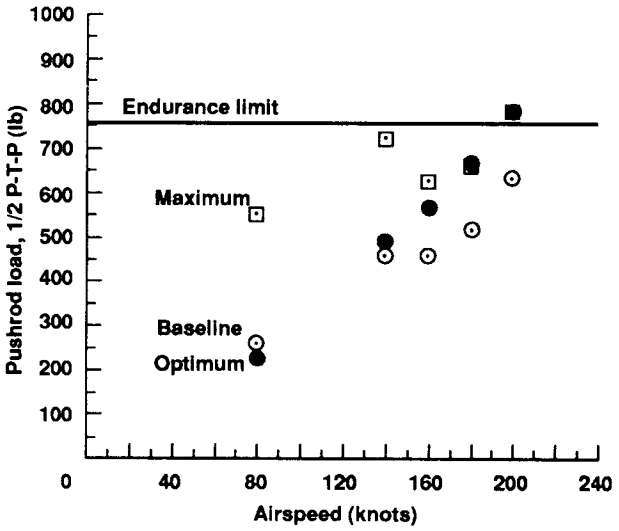

Fig. 5 Pushrod load variation with 1 deg 3P HHC input, S-76, 10,000 lb.

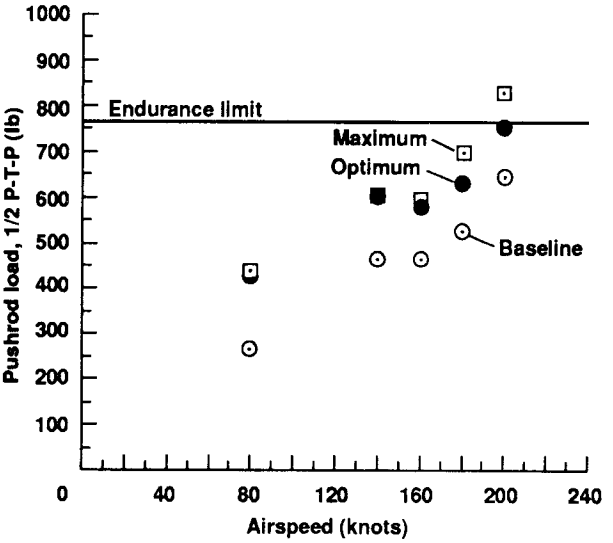

Fig. 7 Pushrod load variation with 1 deg 5P HHC input, S-76, 10,000 lb.

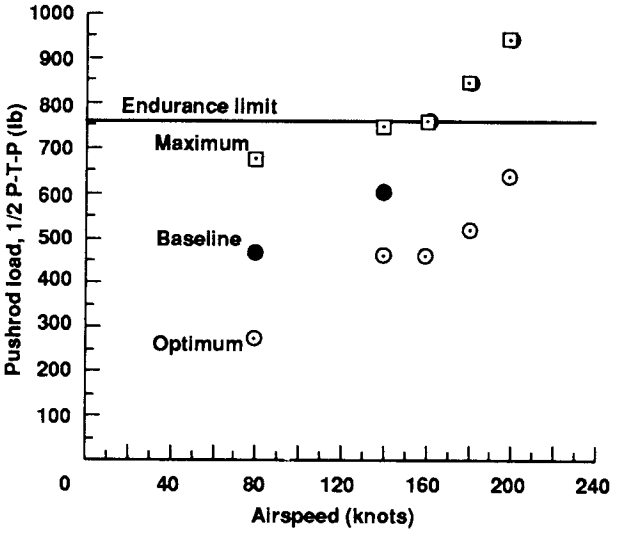

Fig. 6 Pushrod load variation with 1 deg 4P HHC input, S-76, 10,000 lb.

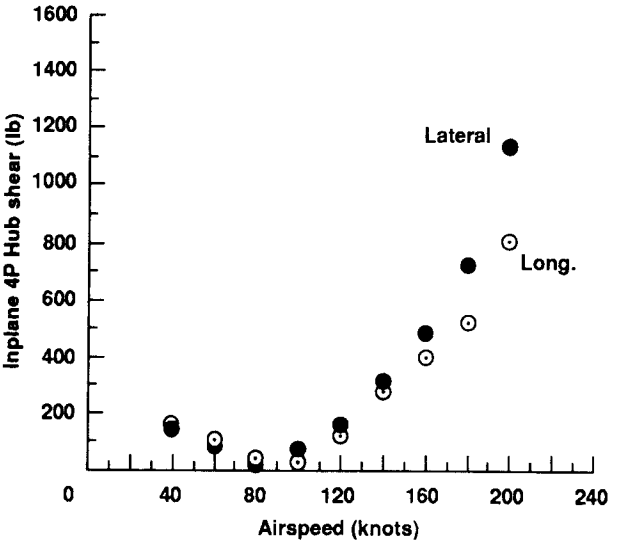

Fig. 8 Variation of inplane hub shears with airspeed, S-76, 10,000 lb.

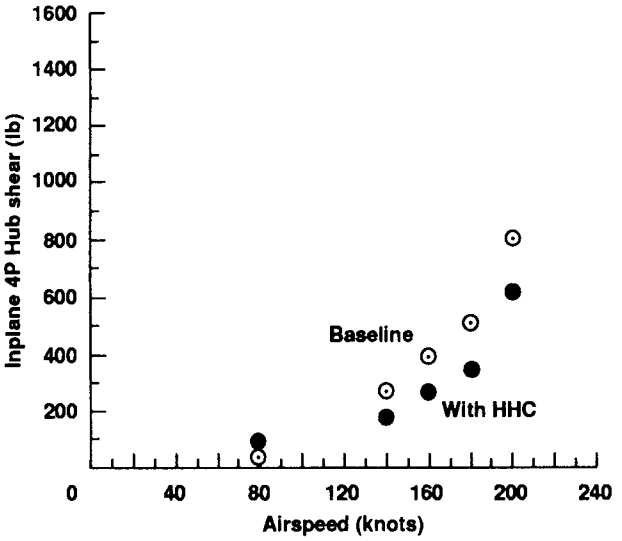

Fig. 9 Effect of optimum 3P HHC input on longitudinal hub shear (HHC amplitude is specified as 1 deg; in this case, optimum phase is 180 deg), S-76, 10,000 lb.

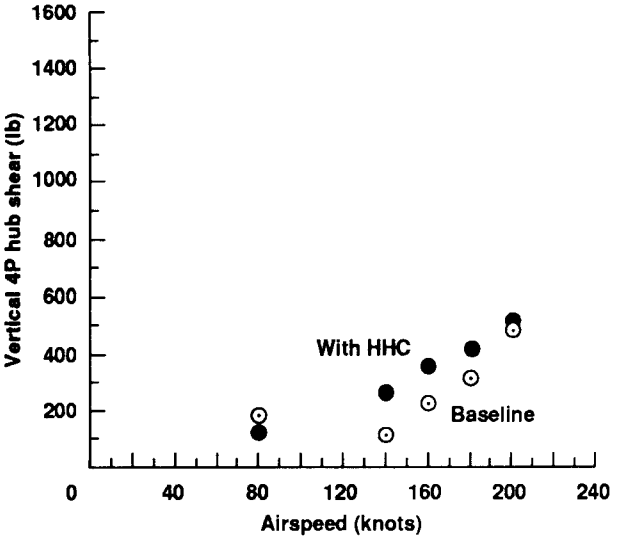

Fig. 11 Effect of "optimum" 3P HHC input on vertical hub shear (HHC amplitude is specified as 1 deg; in this case, "optimum" refers to minimum inplane shears), S-76, 10,000 lb.

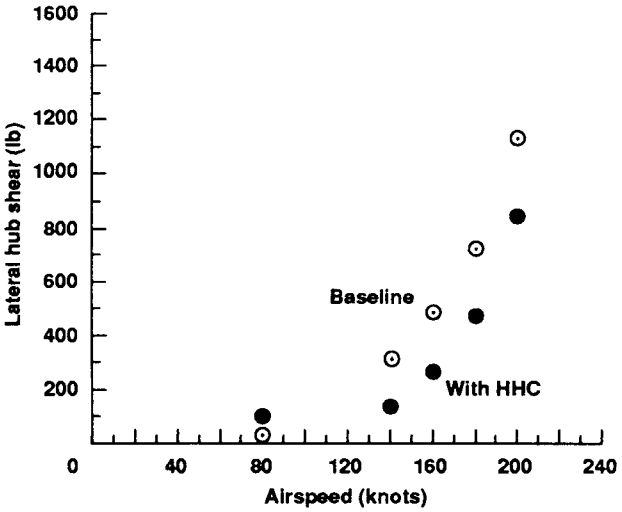

Fig. 10 Effect of optimum 3P HHC input on lateral hub shear (HHC amplitude is specified as 1 deg; in this case, optimum phase is 180 deg), S-76, 10,000 lb.

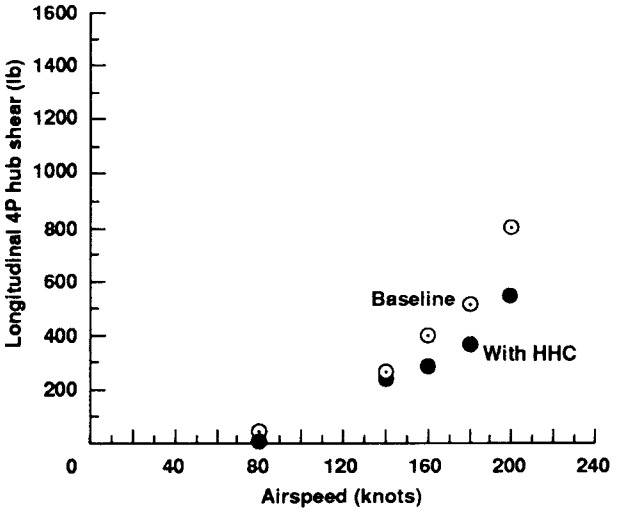

Fig. 12 Effect of optimum 4P HHC input on longitudinal hub shear (HHC amplitude is specified as 1 deg; in this case, optimum phase is 90 deg), S-76, 10,000 lb.

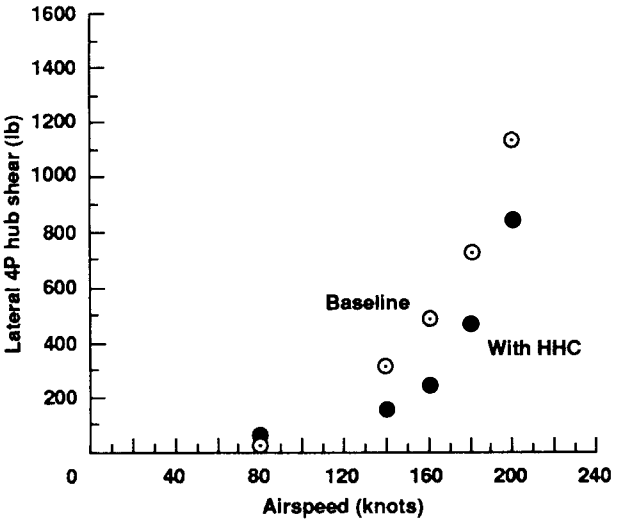

Fig. 13 Effect of optimum 4P HHC input on lateral hub shear (HHC amplitude is specified as 1 deg; in this case, optimum phase is 90 deg), S-76, 10,000 lb.

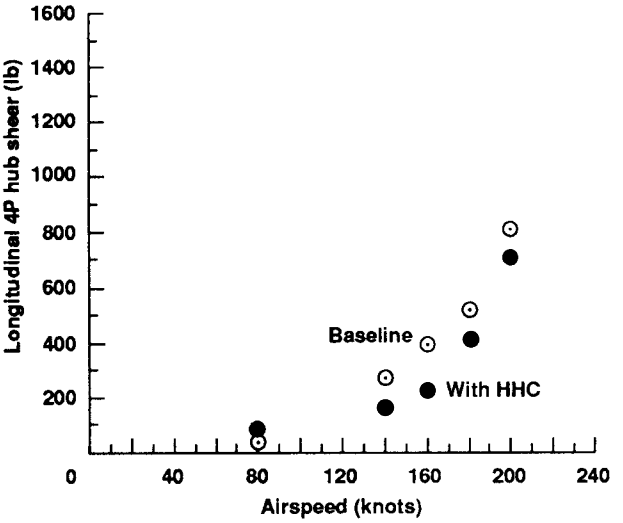

Fig. 15 Effect of optimum 5P HHC input on longitudinal hub shear (HCC amplitude is specified as 1 deg; in this case, optimum phase is 90 deg), S-76, 10,000 lb.

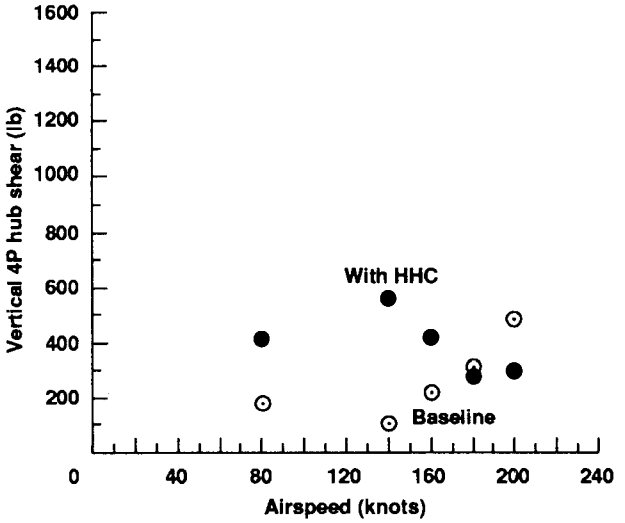

Fig. 14 Effect of "optimum" 4P HHC input on vertical hub shear (HHC amplitude is specified as 1 deg; in this case, "optimum" refers to minimum inplane shears), S-76, 10,000 lb.

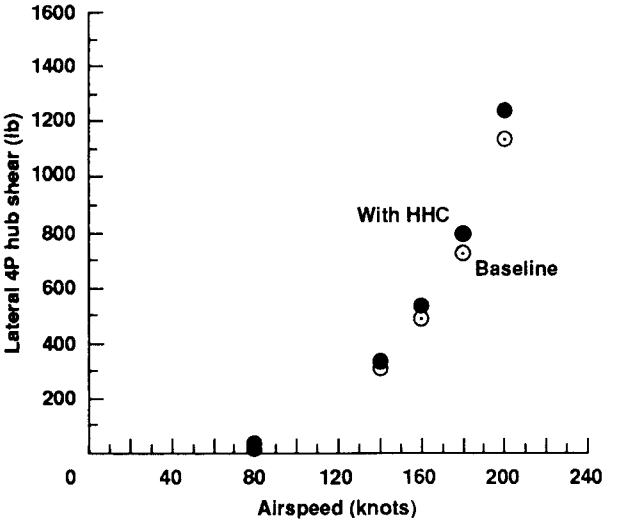

Fig. 16 Effect of "optimum" 5P HHC input on lateral hub shear (HCC amplitude is specified as 1 deg; in this case, longitudinal shear was minimized), S-76, 10,000 lb.

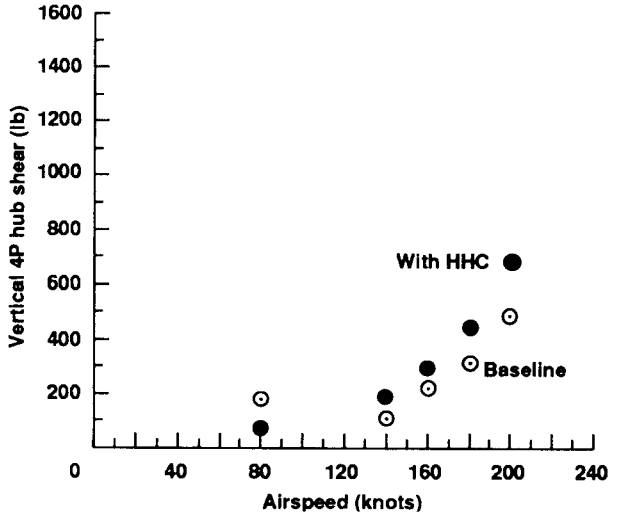

Fig. 17 Effect of "optimum" 5P HHC input on vertical hub shear (HCC amplitude is specified as 1 deg; in this case, longitudinal shear was minimized), S-76, 10,000 lb.

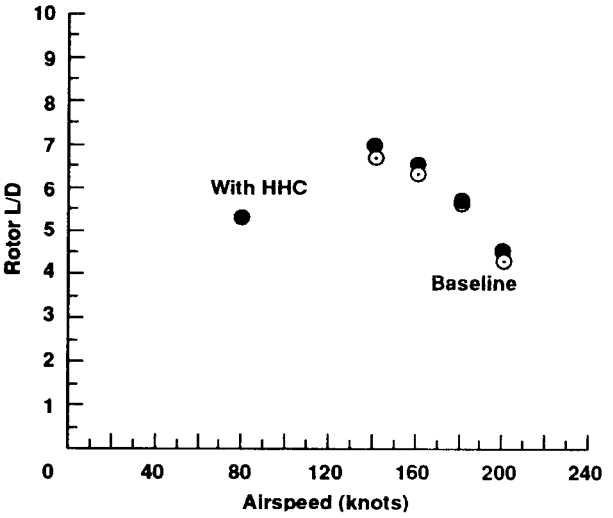

Fig. 19 Effect of "optimum" 3P HHC input on rotor performance ("optimum" input minimizes inplane shears), S-76, 10,000 lb.

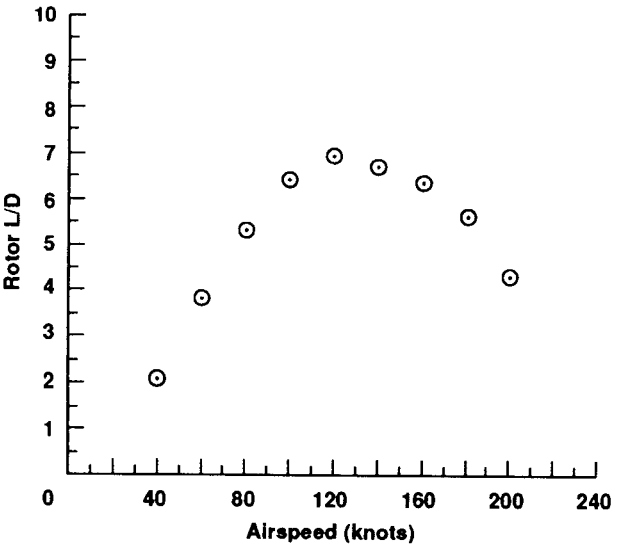

Fig. 18 Variation of rotor performance with airspeed, S-76, 10,000 lb.

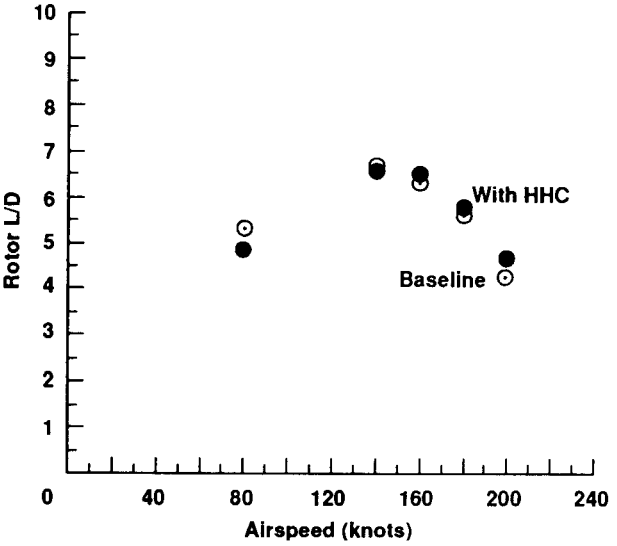

Fig. 20 Effect of "optimum" 4P HHC input on rotor performance ("optimum" input minimizes inplane shears), S-76, 10,000 lb.

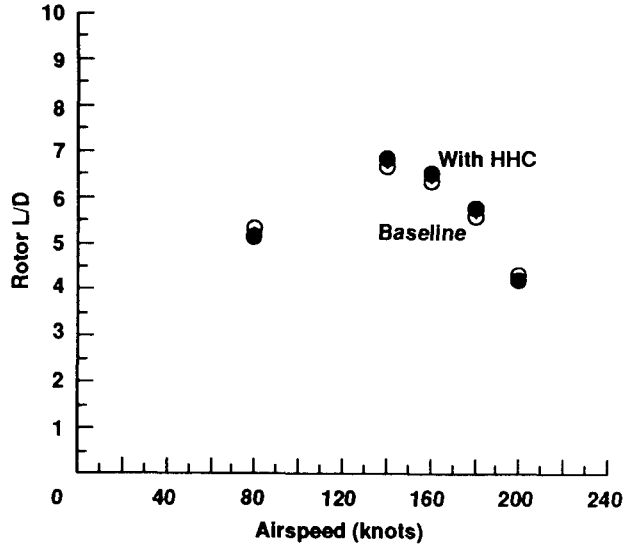

Fig. 21 Effect of "optimum" 5P HHC input on rotor performance ("optimum" input minimizes longitudinal shears), S-76, 10,000 lb.